

Linköping University Postprint

On-axis homoepitaxial growth on Si-face 4H–SiC substrates

J. Hassan, J.P. Bergman, A. Henry and E. Janzén

N.B.: When citing this work, cite the original article.

Original publication:

J. Hassan, J.P. Bergman, A. Henry and E. Janzén, On-axis homoepitaxial growth on Si-face 4H–SiC substrates, 2008, Journal of Crystal Growth, (310), 20, 4424-4429.

<http://dx.doi.org/10.1016/j.jcrysgro.2008.06.081>.

Copyright: Elsevier B.V., <http://www.elsevier.com/>

Postprint available free at:

Linköping University E-Press: <http://urn.kb.se/resolve?urn=urn:nbn:se:liu:diva-15197>

On-axis homoepitaxial growth on Si-face 4H–SiC substrates

J. Hassan, J.P. Bergman, A. Henry and E. Janzén

Department of Physics, Chemistry and Biology, IFM, Linköping University, S-58183
Linköping, Sweden

Abstract

Homoepitaxial growth has been performed on Si-face nominally on-axis 4H–SiC substrates using horizontal Hot-wall chemical vapor deposition system. Special attention was paid to the surface preparation before starting the growth. In-situ surface preparation, starting growth parameters and growth temperature are found to play a vital role to maintain the polytype stability in the epilayer. High quality epilayers with 100% 4H–SiC were obtained on full 2" substrates. Different optical and structural techniques were used to characterize the material and to understand the growth mechanisms. It was found that the replication of the basal plane dislocation from the substrate into the epilayer can be completely eliminated. The on-axis grown epitaxial layers were of high quality and did not show surface morphological defects, typically seen in off-axis grown layers, but had a high surface roughness.

Keywords: A1. Atomic force microscopy; A1. Etching; A3. Hot wall epitaxy; B2. Semiconducting materials; B3. Bipolar transistors

1. Introduction

The superior physical properties of SiC, like wide band gap, high thermal conductivity and high breakdown electric field, make it potentially useful for high power, high temperature and high frequency electronics devices [1]. SiC exists in many different polytypes, such as 4H, 6H, 3C and 15R but 4H-SiC is the polytype of highest interest for high power and high temperature electronics. The difference between different polytypes lies in the stacking sequence of Si-C bilayers along the *c*-axis.

SiC homoepitaxy is a key process for the growth of device quality layers. In order to replicate the substrate polytype into epilayer, off-axis substrate with several degree off-cut typically along the $\langle 11\bar{2}0 \rangle$ direction is commonly used. The high density steps on the surface provide unique sites for the adatoms and growth is followed through step-flow growth inheriting the stacking sequence of the substrate [2]. This technique is successfully used to grow homoepitaxial layers of 4H-SiC with specular surface morphology.

However, there are several problems related to off-axis growth. First, with the increasing diameter of the bulk crystal, off-axis sliced wafers from an on-axis growth boule result in more material losses [3]. Second, the growth on off-axis substrates results in the replication of basal plane dislocations (BPDs) from the substrate into the epilayer. In the case of high power bipolar electronic devices, the BPDs are reported to act as source of expanding stacking faults formation in the basal plane during bipolar injection [4-5]. These stacking faults result in an increased forward voltage drop and thus in bipolar degradation. There have been several reports showing that most of the BPDs convert into threading edge dislocations (TEDs) during epitaxial growth [6-9] which are less harmful for bipolar devices. Also, different epitaxial techniques have been used to further enhance the conversion of BPD into TED at the epi-substrate interface [10,11] but still the total number of dislocations in the epilayer is the same as in the substrate.

Third, during growth on off-axis substrates the step-flow growth mechanism is dominant [12]. When, during epitaxial growth, the step-flow growth interacts with spiral growth around screw dislocations, it may give rise to new structural defects in the epilayer [13]. In the case when defects originate and extend along the basal plane, they will cover a large area of the epilayer surface. Several studies have shown that such large area extended defects, replicating from substrate into epilayer or originating at epilayer-substrate interface, are detrimental to devices [14]. Homoepitaxial growth on 4H-SiC on-axis substrate could be a useful approach to overcome most of these problems. The crystal structure of 4H-SiC on $\{0001\}$ Si-face is similar to that of 3C-SiC on (111) face and at normal epitaxial growth temperatures 3C growth is thermodynamically preferred unless there are enough steps on the substrate surface that can help replicating the polytype of the substrate.

There have been several reports on epitaxial growth on nominally on-axis 4H and 6H-SiC substrates [15-18]. Among those only one with successful homoepitaxy; however, the work was conducted on C-face substrates [19]. C-face seed crystals are generally used for the bulk growth of 4H-SiC while bulk growth using Si-face seed crystals often results in switching of polytype to 6H-SiC [20]. This shows that the C-face has better polytype stability for 4H-SiC growth. However, epitaxial growth on C-face is of less interest, especially for high power devices, due to higher n-type background doping of the active device layer and bad control on high doping of p-type contact layer.

Epitaxial growth on Si-face usually results in a random nucleation of 3C–SiC inclusions along with 4H–SiC [21-23]. Formation of 3C–SiC inclusions on Si-face substrate is attributed to the high surface energy, low surface diffusion length of the adatoms and surface roughness. In this study, we have performed homoepitaxial growth on Si-face on-axis substrate in a horizontal Hot-wall chemical vapor deposition reactor (HWCVD) [24] using in-situ surface preparation and improved starting growth parameters in combination with relatively high growth temperature.

2. Experiments

All the samples used were commercially obtained and nominally on-axis, Si-face polished 4H–SiC. The samples were either full 2" wafers or small pieces cut from 3" wafers. A HWCVD [24] was used for homoepitaxial growth. Hydrogen purified through heated palladium membrane was used as carrier gas. Silane and propane gases were used as sources of Si and C, respectively, while nitrogen and trimethylaluminum were used as n- and p-type dopants, respectively. The growth temperature, as measured by the pyrometer facing the ceiling of the susceptor, was typically 1620 °C with a growth pressure of 200 mbar. The typical gas flow rates are 18.46 ml/min of SiH₄ and 10.27 ml/min of C₃H₈ diluted in 57 l/min of H₂, keeping C/Si=1. A series of samples with epilayer thickness of 10–40 μm were grown with a growth rate of 3 μm/h. Typical net background impurity level was in the high 10¹³ cm⁻³ range with n-type conductivity. Intentional doping was between 5×10¹⁴ cm⁻³ and 5×10¹⁸ cm⁻³ for n-type layers and was between 1×10¹⁵ cm⁻³ and 5×10¹⁹ cm⁻³ for p-type layers. In-situ surface preparation [25], prior to the growth, was performed under Si-rich conditions for 20 min at 1620 °C. The off angle of the substrates were measured by high resolution X-ray diffraction (HRXRD) using a Philips 'X-Pert' XRD setup. The doping of the epilayer was measured either by CV measurements with mercury probe or by the relative intensity of the nitrogen bound exciton (N-BE) no-phonon line and one of the free exciton (FE) lines in the low temperature photoluminescence (PL) spectrum of the near band gap (NBG) region [26]. The PL excited either by 244 nm or by 351 nm Ar⁺ laser line was dispersed by a single monochromator on which a UV sensitive CCD camera cooled with liquid nitrogen was mounted to rapidly detect the PL spectra.

The surface morphology of both substrate and epilayer was observed using optical microscopy with Nomarski diffractive interference contrast. The detailed surface step structure and surface roughness was measured using Dimension 3100 atomic force microscope (AFM) with tapping mode. The polytype identification was done using HRXRD or illumination of epilayer under defocused UV laser light at 77 K. Also PL mapping at liquid helium temperature was performed to identify the presence of any other polytype or residual impurity. In order to reveal the dislocations intersecting the surface, the sample was etched in molten KOH at 500 °C for 5 min. Synchrotron white beam X-ray topography (SWBXT) was performed using the synchrotron radiation source HASYLAB-DESY Hamburg. SWBXT was made in back reflection mode on some selected areas of the samples.

3. Results and discussion

3.1. *In-situ surface preparation*

A clean surface with reduced number of surface damages is the key to produce defect free homoepitaxial layers [27]. As received SiC samples are known to have polishing-related damages. It has been shown previously that, in the case of growth on Si-face on-axis substrate, the 3C–SiC inclusions originate at epi–substrate interface and mainly at substrate surface damages or at larger macro-steps and continue to grow laterally in the epilayer and finally cover large area of the surface. In-situ etching, under C-rich conditions, prior to the epitaxial growth is a well-known process to reduce the surface damages. In the case of off-cut substrate, C-rich condition during temperature ramp-up has also been shown to reduce the depletion of surface C which helps to prevent the condensation of Si into Si-droplets [28] and [29]. We have performed in-situ etching using different ambient conditions such as etching in pure hydrogen, in a mixture of hydrogen and propane (carbon-rich condition) and in a mixture of hydrogen and silane (silicon-rich conditions) details of which can be found elsewhere [25]. Additional propane or silane (25% and 20%, respectively, of the flows normally used for SiC growth) was introduced just before the temperature inside the susceptor reached the melting point of Si. The etching was performed at 1620 °C for 20 min and the etching period was started during temperature ramp-up when the temperature reached 1550 °C. Etching, under all conditions, resulted in the removal of all polishing-related damages and the surface appears with step bunching which is attributed to the high surface energy of the Si-face. An example of Si-face sample etched in Si-rich conditions is given in Fig. 1a. Defect selective etching resulted in the formation of two-step deep round and hexagonal etch pits around some of the dislocations under all ambient conditions while the density of the defect selective etch pits was found to be higher on the sample etched under pure hydrogen and under Si-rich conditions as compared to that etched under C-rich conditions.

Etching in pure hydrogen resulted in the formation of zigzag-shaped macro-steps. C-rich condition resulted in the formation of broken, non-linear and irregularly spaced macro-steps. Etching under Si-rich condition, produced linear, continuous and regularly spaced macro-steps on the surface. AFM images taken with tapping mode showed a smaller height and uniformly distributed macro-steps on the sample etched under Si-rich condition compared to that etched under pure hydrogen and under C-rich condition also, the surface roughness was lowest on the sample etched under Si-rich condition. AFM analysis of the whole surface of all samples showed that all of the screw dislocations opened up in the form of shallow etch pits with typical hexagonal spiral geometry as shown in Fig. 1b. The micro-steps originating from the screw dislocations cover the entire surface and the height of the micro-steps is equal to unit cell height, i.e., 1 nm in the case of 4H–SiC. The high density of micro-steps acts as a sink for the incoming atoms to the surface and replicate the polytype information from substrate into the epilayer.

Under pure hydrogen ambient conditions, Si-droplets are known to form on the surface of off-cut substrate during in-situ etching and even during temperature ramp-up. Such behavior was not observed on the surface of on-axis substrate even under etching in Si-rich conditions. Similar behavior was found on both Si- and C-face substrates regarding Si-droplets. This could be attributed to the low step density on the surface of on-axis substrate which may results in a low partial pressure of Si on on-axis substrate surface as compared to that on off-

cut substrate under the same conditions. The experimental evidence showed that the in-situ etching under Si-rich conditions effectively removed the surface damages and produced homogeneous step structure with lowest surface roughness on Si-face on-axis substrate surface even if the etch pits density was higher than under C-rich conditions. Therefore, in-situ etching under Si-rich conditions was preferred and used for all the growth experiments reported here.

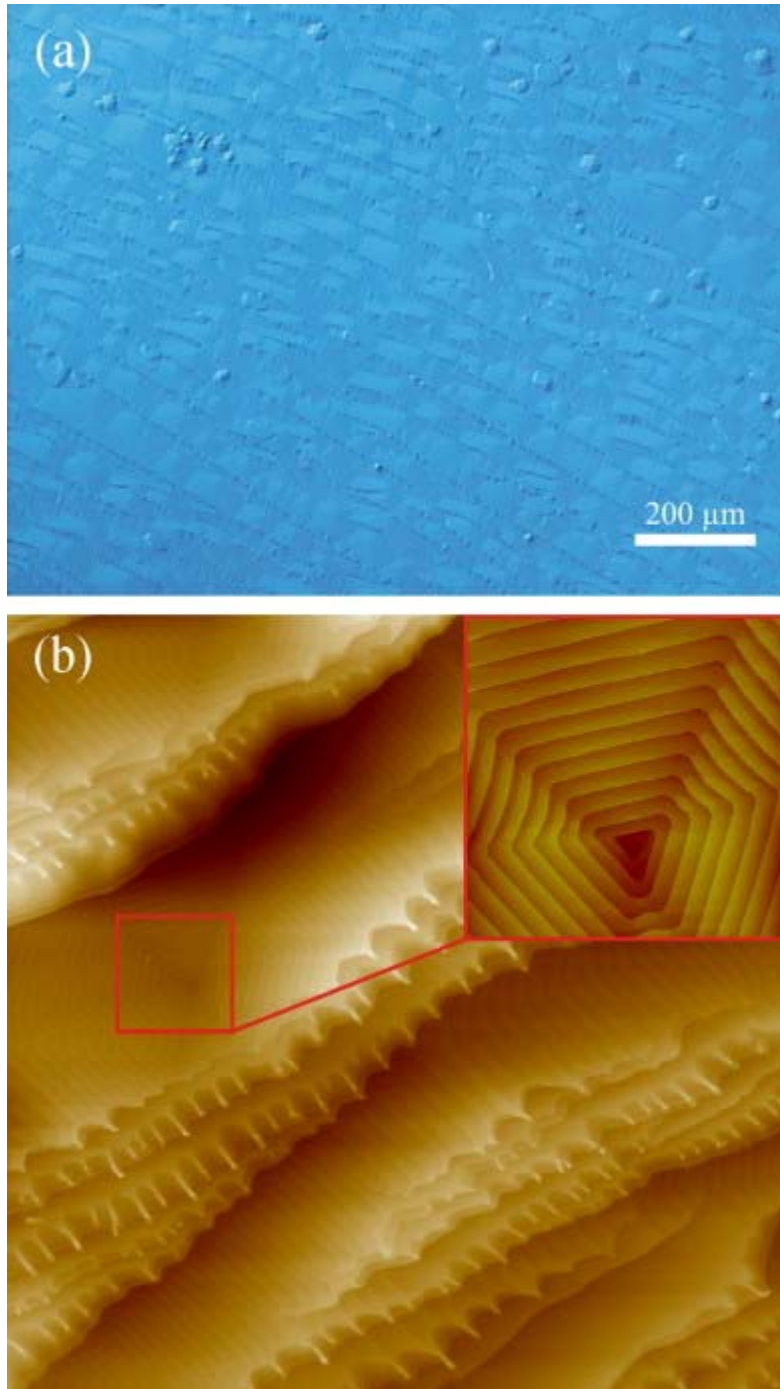


Fig. 1. (a) Optical image taken from the Si-face sample etched in Si-rich conditions and (b) a $(75 \times 75) \mu\text{m}^2$ AFM image taken from the same sample while the inset is a $(15 \times 15) \mu\text{m}^2$ scan taken around a shallow etch pit.

3.2. Starting growth parameters

Starting growth parameters play a vital role in the homoepitaxial growth. Most of the defects, including 3C inclusions, nucleate at the substrate–epi interface and continue to grow in the epilayer. Any abrupt change, at the beginning of the growth, in the gas phase may result in the formation of such defects. Therefore, after in-situ etching it is important to change the growth mode from negative growth (etching) to positive growth very slowly and gradually. A very low supersaturation at the beginning of the growth avoids the 2D nucleation of 3C–SiC on wide terraces and the polytype of the substrate replicates into epilayer through preferential growth at the steps produced by the screw dislocations. The growth was started with a very low concentration of the precursors with C/Si=1, at the inlet of the susceptor. After the substrate is covered with a few hundreds nm of high purity homoepitaxial layers, stable growth can be continued using a higher growth rate. The flow rate of the precursors was gradually increased during 20 min, to avoid any abrupt change in the gas phase, to obtain a stable growth rate of 3 $\mu\text{m/h}$.

3.3. Effect of the growth temperature

Epitaxial layers, on off-cut substrates, are normally grown in the temperature range of 1500–1580 °C. On off-cut substrates, the step density is high and at the given temperature range the adatom diffusion length is high enough to incorporate at a suitable lattice site to reproduce the substrate polytype into the epilayer. In the case of nominally on-axis substrate, depending on the small off-cut typically 0.08° as measured on our samples, the step density produced by the minor off-cut is very low. Therefore, homoepitaxial layers grown on nominally on-axis Si-face substrate show a columnar growth, at the screw dislocations intersecting the surface, following the spiral growth mode. Such features appear on the surface as a result of low adatom surface diffusion length. The adatom surface mobility can be increased by increasing the growth temperature. Growth at high temperature also enhances re-evaporation of any unstable 3C nuclei along with other defects formed at the epi–substrate interface. Increased adatom diffusion length at high temperature will on the other hand increase the probability of the adatom to reach the suitable lattice site.

Fig. 2a shows a PL image taken at 77 K under UV illumination, from a 10 μm thick epitaxial layer grown on Si-face on-axis substrate at the growth temperature of 1560 °C. The 3C inclusions, appeared as black spots in this image and are highlighted with dotted white lines, lie parallel to the macro-steps. This geometry indicates that the 3C inclusions are nucleating and expanding parallel to the macro-steps. In some cases, on thick epilayers, 3C inclusions are also seen to expand along the off-cut direction due to the nature of the step-flow growth mode but were not observed to expand in step-up direction. These inclusions are assumed to nucleate during the growth. Another 10 μm thick epilayer was grown under the same conditions but at relatively higher growth temperature of 1620 °C. PL image taken at 77 K under UV illumination had a homogenous emission without any 3C-related dark spots. Also, low temperature PL spectral mapping showed only 4H-related spectra without any 3C-related emissions in the spectrum. An optical image taken from this epilayer is shown in Fig. 2b.

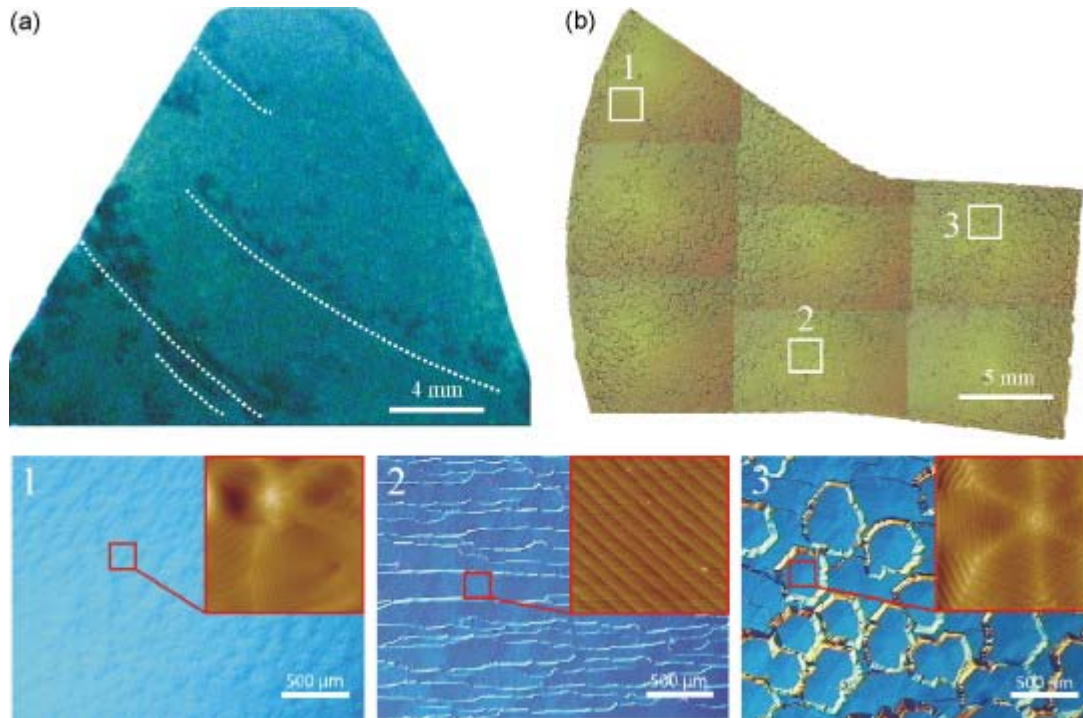


Fig. 2. (a) PL image taken under UV illumination at 77 K from a 10 μm thick epilayer grown at 1560 $^{\circ}\text{C}$ and (b) optical image taken from a 10 μm thick epilayer grown at 1620 $^{\circ}\text{C}$. The high magnification images taken from the area marked with 1, 2 and 3 in (b) are shown below. The high magnification AFM images are shown as inset.

3.4. Growth mechanism

In Fig. 2b, three different kinds of the surface morphologies can be identified, marked with numbers 1–3 and the corresponding high magnification optical images are shown below. In epitaxial growth, growth mechanism mainly depends on the surface structure of the substrate. In the case of normal off-cut substrate, the growth is mainly governed by the step-flow while in the case of ideally on-axis surface spiral growth occurs via micro-steps provided by screw dislocations intersecting the surface [30]. In the case of nominally on-axis substrate, the situation could be entirely different. As it is not possible to get absolutely on-axis surface when slicing a grown boule, there is always a small tilt. Especially in the case of SiC substrate, grown at very high temperatures, there is also a bending of the lattice planes in the wafer which may result in local variation of the surface off-orientation. Therefore, on the same wafer we may have local areas with surface orientation close to perfectly on-axis and local areas with surface orientation with a small off-cut. From our HRXRD measurements of the wafers used in this study, we have observed a small variation in the off-cut angle of $\pm 0.08^{\circ}$. In the areas where the surface is close to perfectly on-axis, spiral growth mechanism is dominant as can be seen in the high magnification optical images from areas marked as ‘1’ and ‘3’ in Fig. 2b. The columnar growth in the area ‘3’ is probably due to low dislocation density in this area as compared to in the area ‘1’. Also, the surface roughness, as measured with AFM in tapping mode, is higher in the area ‘3’ (RMS value of about 40 nm for $100 \times 100 \mu\text{m}$ scan) as compared to that in the area ‘1’ (RMS value of about 4 nm for $100 \times 100 \mu\text{m}$ scan). The nearby interacting spirals meet each other perfectly and no defect or foreign polytype inclusions were found at the interfaces. AFM image taken from area ‘3’, seen in the inset, shows that the surface is covered with micro-steps of unit cell height with a typical spiral-shaped geometry. In the high magnification image taken from the area ‘2’ step-

flow growth is found to be dominant, probably due to the locally larger but still small off-axis in this area. AFM image taken from this area on a terrace, as seen in the inset, shows that the surface is covered with periodically arranged linear steps of unit cell height. The growth steps, at the beginning of the growth, are supplied by the micro-steps originated from threading screw dislocations intersecting the surface and uncovered during in-situ etching. Under very low supersaturation, the incoming atoms incorporate preferentially at these micro-steps and the growth is started through the spiral growth mode. After the growth of a few tens of nm the micro-steps start to accumulate at the boundaries of macro-steps but the terraces between the macro-step are still covered with micro-steps of unit cell height. The incoming atoms incorporate at the micro-steps and in this way the macro-steps keep advancing in the off-cut direction on the terraces of the lower steps while the micro-steps follow the crystallographic orientation of the original spiral and the growth mode switches to the step-flow growth mode.

3.5. Surface morphology and purity of the epilayers

A 40 μm thick epitaxial layer grown on Si-face, on-axis, 2" full wafer, under the growth conditions described above, showed 100% replication of the substrate polytype into the epilayer. The polytype identification was primarily done by the illumination of full wafer, immersed in liquid nitrogen, under UV light as shown in Fig. 3a. No sign of 3C-SiC inclusions was seen, not even at the edges of the wafer. In order to examine the purity of the epilayer, low temperature PL mapping was performed of the entire wafer. The PL spectrum, taken from the middle of the wafer, shown in Fig. 3b, in the energy range of 3.3–2.1 eV does not show the presence of any foreign polytype. Similar PL spectra were observed over the whole wafer, even close to the periphery. The PL spectrum is dominated by the NBG

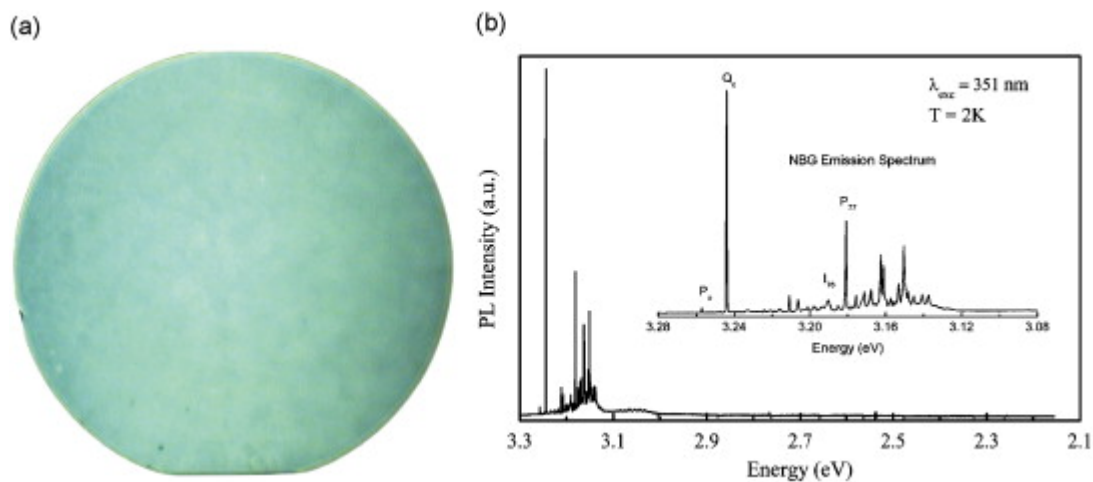


Fig. 3. (a) PL image taken under UV illumination at 77 K from a full 2" wafer with 40 μm thick epilayer and (b) PL spectrum taken at 2 K at close to the center of the wafer, the inset shows the characteristic NBG emission spectrum.

emission where the N-BE and FE lines can be observed. The inset in fig. 3b shows characteristic NBG spectrum. As the layer was intentionally doped, the intensity of N-BE is higher than the FE peak. For low-doped material with nitrogen concentration lower than $3 \times 10^{16} \text{ cm}^{-3}$, the relative intensity between the N-BE no-phonon line, such as Q_0 in 4H-SiC and one of the FE lines, such as I_{76} the strongest phonon replica of the FE, has allowed a quantitative estimation of the doping concentration [26]. The concentration of the nitrogen

for this doped layer determined by PL is $3 \times 10^{15} \text{ cm}^{-3}$. Fig. 4a shows an optical image taken from the middle of the wafer. AFM analysis showed that the surface roughness is increasing with increasing thickness of the epilayer. The macro-step height, as found by AFM, could reach over 100 nm for 40 μm thick epilayer without giving rise to the nucleation of 3C-SiC inclusions. The epilayer growth is continued through the steps produced by threading screw dislocations on the surface, as shown in Fig. 4b.

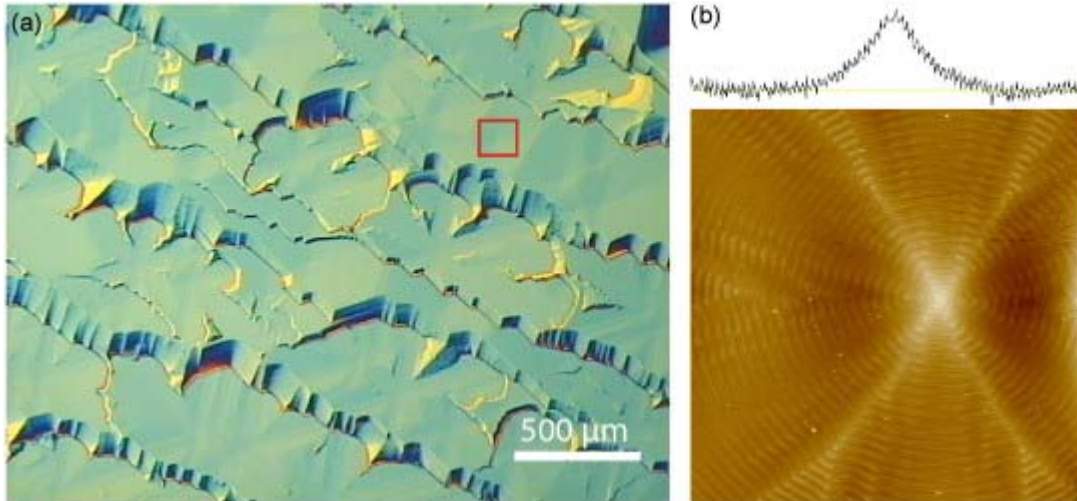


Fig. 4. (a) Optical image taken at the middle of the wafer and (b) a $(50 \times 50) \mu\text{m}^2$ AFM scan taken from the area marked in (a).

3.6. Structural defects

The HRXRD analysis of the epilayer also confirms the 100% replication of the substrate polytype into the epilayer and no 3C or any other foreign polytype-related reflection was observed in $2\theta-\omega$ scan. In the case of homoepitaxial growth on off-cut substrate BPD conversion into TED, at epi-substrate interface, is a well-known process [6-9]. Though, in this process, the total number of BPD in the epilayer is reduced but still the total number of dislocations is the same as that in the substrate. One of the main reasons for growing homoepitaxial layers on on-axis substrate was to eliminate the BPD propagation from the substrate into the epilayer; in this way the total number of defects can be reduced in the epilayer. Optical images taken from the KOH etched surface do not show BPD-related etch pits on the surface, one such example is given in Fig. 5. The on-axis epitaxial growth will naturally avoid the propagation of BPDs from the substrate. BPDs dislocations can also be introduced during the epitaxial growth but were not observed on the surface. The surface morphology and polytype stability of the epilayer remains unaffected for both n- and p-type doping range given in Section 3. Also, CL images taken from highly doped epilayer do not show any sign of double stacking faults. Probably this doping range is too low to give rise to stacking fault formation [31].

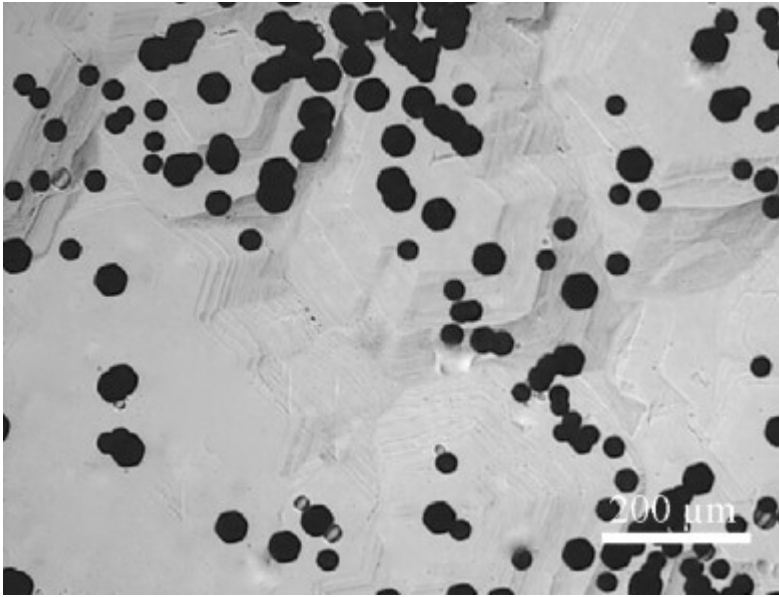


Fig. 5. Optical image taken from the epilayer after etching in molten KOH.

Epilayers grown on off-cut substrate are also known to have some typical epi-defects like triangular defects, half moon, carrots and growth-related pits on the surface. Preliminary studies based on optical microscopy and SWBXT show that the epilayers grown on Si-face on-axis substrate do not show such kind of surface or structural defects. In-grown basal plane stacking faults are another kind of structural defects which are often present in epilayers grown on off-cut substrate. CL study on on-axis grown epilayers do not show any basal plane stacking faults. The absence of surface morphological defects could be attributed to the better surface preparation during in-situ etching and stable starting growth parameters. Apart from the absence of surface defects, the surface roughness is quite high as compared to the epilayers grown on the off-cut substrates.

4. Conclusions

On-axis epitaxial growth with 100% polytype replication has been performed on a full 2" 4H-SiC wafer. In-situ surface preparation has been shown to be a key process for homoepitaxial growth on Si-face on-axis substrate. Si-rich conditions are found to be better to remove the polishing-related surface damages and to get uniform step structure on the surface with low surface roughness. Also, in-situ etching under Si-rich condition does not result in the formation of Si-droplets on the surface. Screw dislocations act as a continuous source of steps on the surface and growth at relatively high temperature in combination with in-situ etching under Si-rich condition resulted in homoepitaxial epilayers. The grown epilayers are of high quality, free of surface morphological defects except for step bunching and spiral hillocks. More importantly no BPDs are found in the epilayer, which means that the total number of dislocations can be reduced in the epilayer, as compared to the substrate. The on-axis epitaxial growth should hence be a suitable process to grow thick epitaxial layers, for bipolar applications, since the problem with bipolar degradation is avoided by the absence of BPDs.

Acknowledgments

The authors are grateful for the financial support from Norstel AB, Swedish Governmental Agency for Innovation Systems (Vinnova), and Swedish Energy Agency (STEM).

References

- 1 B.J. Baliga, *Physics of Semiconductor Power Devices*, JWS Publishing (1996).
- 2 H. Matsunami and T. Kimoto, *Mater. Sci. Eng.* **R20** (1997), p. 125.
- 3 M. Treu, R. Rupp, H. Brunner, F. Dahlquist and Ch. Hecht, *Mater. Sci. Forum* **981** (2004), p. 457.
- 4 J.P. Bergman, H. Lendenmann, P.Å. Nilsson, U. Lindefelt and P. Skytt, *Mater. Sci. Forum* **353–356** (2001), p. 299.
- 5 H. Lendenmann, F. Dahlquist, N. Johansson, R. Söderholm, P.A. Nilsson, J.P. Bergman and P. Skytt, *Mater. Sci. Forum* **353–356** (2001), p. 727.
- 6 S. Ha, P. Mieszkowski, M. Skowronski and L.B. Rowland, *J. Crystal Growth* **257** (2002), p. 244.
- 7 T. Ohno, H. Yamaguchi, S. Kuroda, K. Kojima, T. Suzuki and K. Arai, *J. Crystal Growth* **260** (2004), p. 209.
- 8 Z. Zhang, A. Shrivastava and T.S. Sudarshan, *Mater. Sci. Forum* **527–529** (2006), p. 419.
- 9 Z. Zhang and T.S. Sudarshan, *Appl. Phys. Lett.* **87** (2005), p. 161917.
- 10 J.J. Sumakeris, J.P. Bergman, M.K. Das, C. Hallin, B.A. Hull, E. Janzen, H. Lendenmann, M.J. O'Loughlin, M.J. Paisley, S. Ha, M. Skowronski, J.W. Palmour and C.H. Carter, *J. Mater. Sci. Forum* **527–529** (2006), p. 141.
- 11 Z. Zhang, E. Moulton and T.S. Sudarshan, *Appl. Phys. Lett.* **89** (2006), p. 81910.
- 12 T. Kimoto, H. Nishino, W.S. Yoo and H. Matsunami, *J. Appl. Phys.* **73** (1993), p. 726.
- 13 H. Tsuchida, I. Kamata and M. Nagano, *J. Crystal Growth* **310** (2008), p. 757.
- 14 T. Okada, T. Kimoto, K. Yamai, H. Matsunami and F. Inoko, *Mater. Sci. Eng. A* **361** (2003), p. 67.
- 15 S. Nakamura, T. Kimoto and H. Matsunami, *Mater. Sci. Forum* **457–460** (2004), p. 163.
- 16 P.G. Neudeck, J.A. Powell, G.M. Beheim, E.L. Benavage, P.B. Abel, A.J. Trunek, D.J. Spry, M. Dudley and W.M. Vetter, *J. Appl. Phys.* **92** (2002), p. 2391.
- 17 M. Soueidana, G. Ferroa, B. Nsoulib, F. Cauweta, L. Molleta, C. Jacquiera, G. Younesc and Y. Monteila, *J. Crystal Growth* **293** (2006), p. 433.
- 18 T. Kimoto, Z.Y. Chen, S. Tamura, S. Nakamura, N. Onojima and H. Matsunami, *Jpn. J. Appl. Phys.* **40** (2001), p. 3315.
- 19 K. Kojima, H. Okumura, S. Kuroda and K. Arai, *J. Crystal Growth* **269** (2004), p. 367.
- 20 G. Augustine, H.M.C.D. Hobgood, V. Balakrishna, G. Dunne and R.H. Hopkins, *Phys. Status Solidi B* **137** (1997), p. 202.
- 21 S. Nakamura, T. Kimoto and H. Matsunami, *J. Crystal Growth* **256** (2003), p. 341.
- 22 C. Hallin, Q. Wahab, I. Ivanov, J.P. Bergman and E. Janzén, *Mater. Sci. Forum* **457–460** (2004), p. 193.
- 23 J. Hassan, J.P. Bergman, A. Henry, H. Pedersen, P. J McNally and E. Janzen, *Mater. Sci. Forum* **556–557** (2007), p. 53.
- 24 A. Henry, J. ul Hassan, J.P. Bergman, C. Hallin and E. Janzén, *Chem. Vap. Deposition* **12** (2006), p. 475.
- 25 J. Hassan, J.P. Bergman, A. Henry, E. Janzén, *J. Crystal Growth*, in press.
- 26 I.G. Ivanov, C. Hallin, A. Henry, O. Kordina and E. Janzén, *J. Appl. Phys.* **80** (1996), p. 3504.

- 27 J.A. Powell, J.B. Petit, J.H. Edgar, I.G. Jenkins, L.G. Matus, J.W. Yang, P. Pirouz, W.J. Choyke, L. Clemen and M. Yoganathan, *Appl. Phys. Lett.* **59** (1991), p. 333.
- 28 S. Yu. Karpov, Yu. N. Makarov, M.S. Ramm, Silicon carbide and related materials 1995, in: Proceedings of the Sixth International Conference, 1996, pp. 177–80.
- 29 E. Neyret, L. di Cioccio, E. Blanquet, C. Raffy, C. Pudda, T. Billon and J. Camassel, *J. Mater. Sci. Forum* **338–342** (2000), p. 1041.
- 30 F.C. Frank, *Acta Crystallogr.* **4** (1951), p. 497
- 31 P. Pirouz, M. Zhang, H. McD Hobgood, M. Lancin, J. Douin and B. Pichaud, *Philos. Mag.* **86** (2006), p. 4685.